SCIENTIFIC REPORTS

OPEN

Superconducting H_5S_2 phase in sulfur-hydrogen system under high-pressure

Received: 14 December 2015
Accepted: 01 March 2016
Published: 17 March 2016

Takahiro Ishikawa[1], Akitaka Nakanishi[1], Katsuya Shimizu[1], Hiroshi Katayama-Yoshida[2], Tatsuki Oda[3] & Naoshi Suzuki[4]

Recently, hydrogen sulfide was experimentally found to show the high superconducting critical temperature (T_c) under high-pressure. The superconducting T_c shows 30–70 K in pressure range of 100–170 GPa (low-T_c phase) and increases to 203 K, which sets a record for the highest T_c in all materials, for the samples annealed by heating it to room temperature at pressures above 150 GPa (high-T_c phase). Here we present a solid H_5S_2 phase predicted as the low-T_c phase by the application of the genetic algorithm technique for crystal structure searching and first-principles calculations to sulfur-hydrogen system under high-pressure. The H_5S_2 phase is thermodynamically stabilized at 110 GPa, in which asymmetric hydrogen bonds are formed between H_2S and H_3S molecules. Calculated T_c values show 50–70 K in pressure range of 100–150 GPa within the harmonic approximation, which can reproduce the experimentally observed low-T_c phase. These findings give a new aspect of the excellent superconductivity in compressed sulfur-hydrogen system.

Search for room-temperature superconductors is a challenging study in materials science, and pressurization and hydrogenation have been considered as a way to push up the superconducting critical temperature, T_c, to the higher region[1]. Recently, high T_c superconductivity was experimentally observed in compressed hydrogen sulfide (H_2S) and T_c reaches 203 K at 150 GPa[2,3], which exceeds copper oxide superconductors[4,5] and sets a record for the highest T_c. In the experiments, the superconducting T_c shows 30–70 K in pressure range of 100–170 GPa for the H_2S samples loaded at 100–150 K and compressed to 100 GPa (low-T_c phase) and increases to 203 K for the samples annealed by heating it to room temperature at pressures above 150 GPa (high-T_c phase). The pressure-temperature path dependence of T_c is considered to be involved by changes of stoichiometry from H_2S, but the details have not been identified completely. Therefore, further studies on sulfur-hydrogen system under high-pressure are required for the understanding of the mechanism for its excellent superconductivity.

Stoichiometry, crystal structure, and superconductivity of sulfur-hydrogen system under high-pressure have been investigated by first-principles calculations based on the density functional theory (DFT)[6–17]. Duan *et al.* predicted that H_2S is stable below 43 GPa and decomposes into H_3S and S above the pressure[8]. For H_2S, a monoclinic $P2/c$ structure transforms into a monoclinic Pc structure at 27 GPa. H_3S shows the sequence of pressure-induced structural phase transitions as follows: triclinic $P1 \rightarrow$ orthorhombic $Cccm$ (37–111 GPa) $\rightarrow$ trigonal $R3m$ (111–180 GPa) $\rightarrow$ cubic $Im\text{-}3m$. Other hydrogen-rich stoichiometries, H_4S, H_5S, and H_6S, were reported to be unstable up to at least 300 GPa[8]. Errea *et al.* predicted the stabilizations of HS_2 above 200 GPa and HS above 300 GPa by including zero-point energy[9]. HS_2 crystallizes in a monoclinic $C2/c$ and it transforms into a monoclinic $C2/m$ above 250 GPa. HS takes a monoclinic $C2/m$. Recently, energetically competitive stoichiometries, H_2S_3, H_3S_2, and H_4S_3 were identified[14]. H_2S_3 and H_3S_2 are unstable above 25 and 34 GPa, respectively, whereas H_4S_3 is thermodynamically stable in pressure range from 25 to 113 GPa, in which an orthorhombic $P2_12_12_1$ structure is formed in pressure range of 25–60 GPa and an orthorhombic $Pnma$ in 60–113 GPa.

For the superconductivity, T_c calculated for $Im\text{-}3m$ H_3S with the inclusion of anharmonic effects shows 194 K at 200 GPa[9,10], which is in good agreement with recent results of synchrotron x-ray diffraction measurements

[1]Center for Science and Technology under Extreme Conditions, Graduate School of Engineering Science, Osaka University, 1–3 Machikaneyama, Toyonaka, Osaka 560-8531, Japan. [2]Graduate School of Engineering Science, Osaka University, 1-3 Machikaneyama, Toyonaka, Osaka 560-8531, Japan. [3]Institute of Science and Engineering, Kanazawa University, Kakuma, Kanazawa, Ishikawa 920-1192, Japan. [4]Department of Pure and Applied Physics, Kansai University, 3-3-35 Yamate, Suita, Osaka 564-8680, Japan. Correspondence and requests for materials should be addressed to T.I. (email: ishikawa@stec.es.osaka-u.ac.jp)

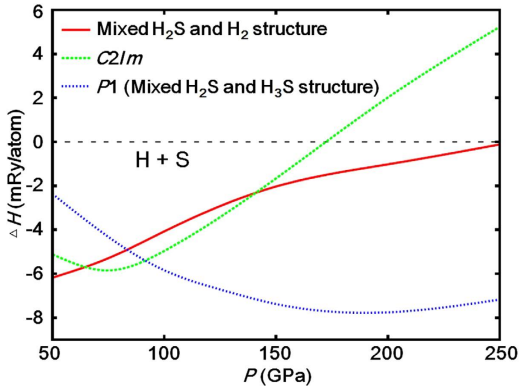

Figure 1. Formation enthalpy per atom, *H*, of crystal structures obtained by the application of the GA technique to the H_5S_2 stoichiometry. H_5S_2 takes a disorderly mixed structure of H_2S and H_2 molecules at 50 GPa, and it transforms into a monoclinic *C*2/*m* at 64 GPa and then into a triclinic *P*1 with mixed H_2S and H_3S structure at 92 GPa.

combined with electrical resistance measurements for the high-T_c phase[18]. On the other hand, for *R*3*m* H_3S stabilized below 180 GPa, the calculated T_c is lower by approximately 50 K than the experimentally observed one[9,10,14]. For the low-T_c phase, H_2S has been considered as a candidate, and T_c is predicted to be 30–60 K for pressure range of 130–160 GPa in a triclinic *P*-1 structure and 80–40 K for 160–250 GPa in an orthorhombic *Cmca*[6,11]. However, the calculated T_c dose not completely reproduce the experimental data in the pressure region except for 150–160 GPa. For other stoichiometries, the calculated T_c values of *C*2/*c* HS_2, *C*2/*m* HS_2, *C*2/*m* HS, and *Pnma* H_4S_3 are 23.4 K for the effective screened Coulomb repulsion constant μ^* of 0.16 at 200 GPa[9], 14.9 K at 250 GPa[9], 23.4 K at 300 GPa[9], and 0.75 K at 300 GPa[14], respectively, which are all far from the experimentally observed values.

Results

In the present study, we focus on another stoichiometric compound, H_5S_2, which has hydrogen content between H_2S and H_3S. We first explored stable structures of H_5S_2 by the genetic algorithm (GA) technique and first-principles calculations based on DFT, and then compared formation enthalpy per atom among the obtained structures in pressure range from 50 to 250 GPa (Fig. 1). The formation enthalpy was calculated as follows: $\triangle H = H_{H5S2} - 5/7H_H - 2/7H_S$, where H_{H5S2}, H_H, and H_S are the enthalpies per atom of H_5S_2, pure hydrogen (H), and pure sulfur (S), respectively. At 50 GPa, H_5S_2 takes a disorderly mixed structure of H_2S and H_2 molecules. At 64 GPa, a monoclinic *C*2/*m* structure is stabilized. In this structure, four H atoms form two H_2 molecules, and the other H atoms make covalent bonds with the S atoms (Fig. 2a). The *C*2/*m* structure transforms into a triclinic *P*1 structure at 92 GPa. In this phase, H_5S_2 takes a mixed structure of H_2S and H_3S molecules, between which asymmetric hydrogen bonds are formed (Fig. 2b). This structure is also interpreted as a member of the Magnéli-like crystals reported very recently[19].

Next, we investigated thermodynamic stability of H_5S_2 from the convex hull diagram with respect to the H-S stoichiometric compounds, H_xS_{1-x}. Figure 3a shows the static formation enthalpy per atom of the compounds as a function of x, which is defined as $\Delta H(x) = H(x) - xH_H - (1-x)H_S$, at 112 GPa. The structures of the compounds are as follows: β-Po for S[20], *Pnma* for H_4S_3[14], *P*-1 for H_2S[6], *P*1 for H_5S_2, *R*3*m* for H_3S[7], and *B*2/*n* for H[21]. The results show that H_4S_3 and H_5S_2 are below the line connecting between H_3S and S (dotted line) but H_4S_3 is above the line connecting between H_5S_2 and S. As the results, H_5S_2 and H_3S are the compounds on the convex hull (solid line) and are thermodynamically stable at 112 GPa, whereas H_4S_3 and H_2S are predicted to be decomposed at this pressure. Figure 3b shows the formation enthalpies of $H_4S_3 + H_3S$ and $H_3S + S$ relative to that of H_5S_2 as a function of pressure. H_5S_2 is composed from H_4S_3 and H_3S at 110 GPa ($H_4S_3 + 7H_3S \rightarrow 5H_5S_2$), and is decomposed into H_3S and S at 123 GPa ($3H_5S_2 \rightarrow 5H_3S + S$).

Figure 4 shows electronic band structure and density of states (DOS) for *P*1 H_5S_2 at 112 GPa. Antibonding bands formed by hybridization of S 3*p* and H 1*s* states, pushed up in the energy owing to the high pressure, appear as flat band dispersions at the Fermi level (E_F) at around the Γ symmetry point by overlapping conduction bands. As the results, DOS at E_F, *i.e.* $N(E_F)$, is increased and H_5S_2 is a good metal. The hybridization is remarkable at E_F, similar to the cases of H_2S and H_3S predicted earlier[6,7,12], whereas for a ratio of the H 1*s* state to $N(E_F)$ there is a clear distinction among the compounds: $N_H(E_F)/N(E_F) \approx 0.50$ for H_3S at 130 GPa[7], $N_H(E_F)/N(E_F) \approx 0.45$ for H_5S_2 at 112 GPa, and $N_H(E_F)/N(E_F) \approx 0.25$ for H_2S at 130 GPa[6]. Therefore, H_5S_2 and H_3S show a larger contribution of H to the electrons at E_F than H_2S.

We investigated the superconductivity of metallic *P*1 H_5S_2 within the harmonic approximation. Table 1 lists electron-phonon coupling constant λ, logarithmic-averaged phonon frequency ω_{log}, and T_c calculated for *P*1 H_5S_2. The calculated T_c values show 70.1–79.1 K for $\mu^* = 0.13$ and 58.3–66.5 K for $\mu^* = 0.17$ in pressure region of 112–130 GPa, which is close to the data for the experimentally observed low-T_c phase. We also list the similar data for *P*-1 H_2S[6,11] at 130 GPa considered as a candidate of the low-T_c phase. The ω_{log} value of *P*1 H_5S_2 is almost identical to that of *P*-1 H_2S, whereas the λ value *P*1 H_5S_2 is almost 1.5 times as large as that of *P*-1 H_2S. The larger λ value is considered to be involved by the larger contribution of H to the electrons at E_F as mentioned above. As the results, T_c of *P*1 H_5S_2 is higher by approximately 40 K than that of *P*-1 H_2S.

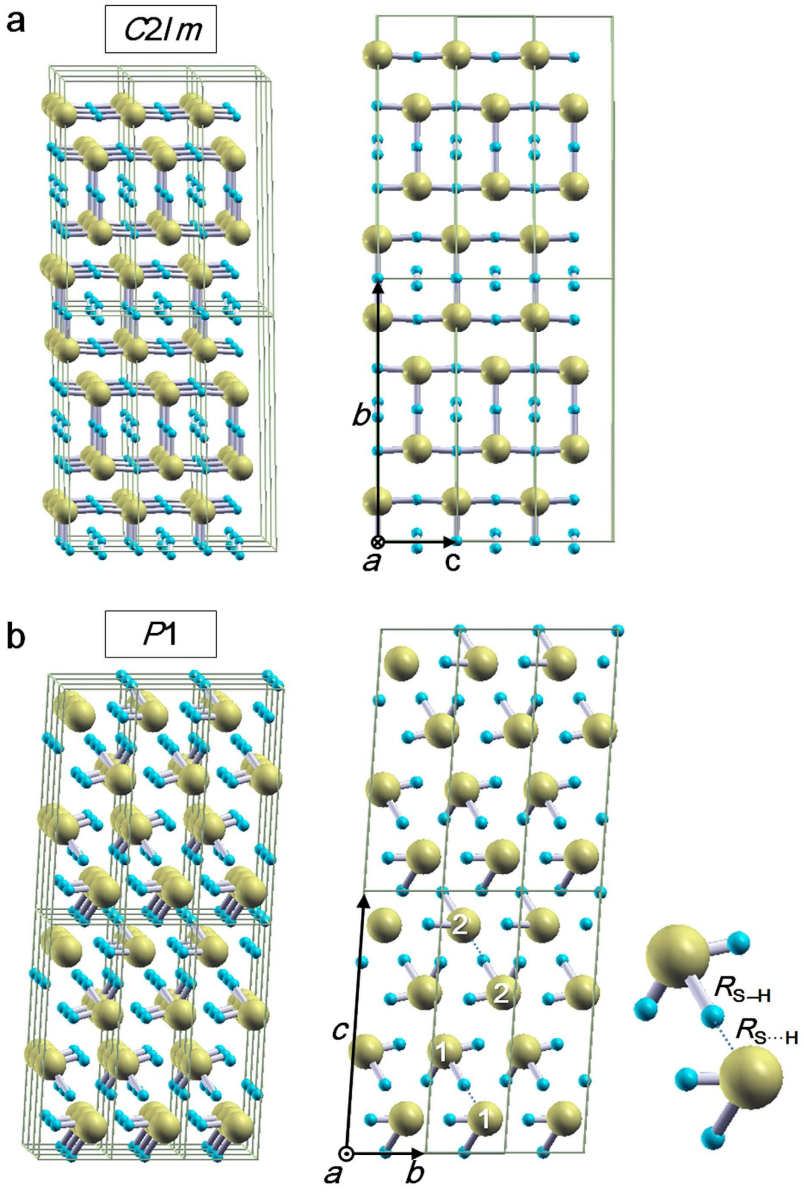

Figure 2. Crystal structures obtained by the GA technique. (**a**) A monoclinic *C*2/*m*. The lattice parameters at 75 GPa are as follows: $a = 2.1813$Å, $b = 10.5741$Å, $c = 3.0907$Å, and $\gamma = 77.563°$. The S atoms occupy a 4i site with (0.1420, 0.8507, 0), and the H atoms a 2a site and two 4i sites with (0.4323, 0.4710, 0) and (0.1476, 0.3429, 0). (**b**) A triclinic *P*1 with a mixed structure of H_2S and H_3S molecules. The lattice parameters at 112 GPa are $a = 2.7127$Å, $b = 2.7119$Å, $c = 8.6105$Å, $\alpha = 84.706°$, $\beta = 84.447°$, and $\gamma = 71.868°$. All the atoms occupy 1a sites: (0.1869, 0.1539, 0.3865), (0.2812, 0.2819, 0.8685), (0.7196, 0.7232, 0.1301), and (0.8252, 0.8495, 0.6114) for S, and (0.6031, 0.5675, 0.7345), (0.7238, 0.8394, 0.8735), (0.1554, 0.2735, 0.1260), (0.0269, 0.9946, 0.9939), (0.7166, 0.5739, 0.4144), (0.2905, 0.4248, 0.5862), (0.0626, 0.0306, 0.7276), (0.9602, 0.9548, 0.2744), (0.4342, 0.4268, 0.2592), and (0.5163, 0.4870, 0.0020) for H. Asymmetric hydrogen bonds are formed between the H_2S and H_3S molecules: (1) $R_{S-H} = 1.4886$Å and $R_{S\cdot H} = 1.5929$Å, and (2) $R_{S-H} = 1.4441$Å and $R_{S\cdot H} = 1.6596$Å, where the numbers in parenthesis correspond to those represented on the S atom and *R* shows the distance between S and H.

We plotted the T_c values obtained at $\mu^* = 0.17$ for *P*1 H_5S_2 with the earlier-predicted T_c data for the H_2S[6,11], H_3S[7,10,11], H_4S_3[14], and HS_2[9] compounds and compared it with the experimental data[3] (Fig. 5). Phonon calculations indicate that *P*1 H_5S_2 is mechanically stable to at least 150 GPa (Fig. 6) and is expected to sustain as a metastable phase above 122 GPa owing to high kinetic barrier, rigid grain boundary, *etc.* The T_c value shows 49.5 K at 100 GPa, slightly increases with pressurization, and reaches 71.8 K at 150 GPa, which are in good agreement with the experimental data below 170 GPa in the low-T_c phase. These results suggest that *P*1 H_5S_2 is a better candidate for the low-T_c phase than H_2S, H_4S_3, and HS_2.

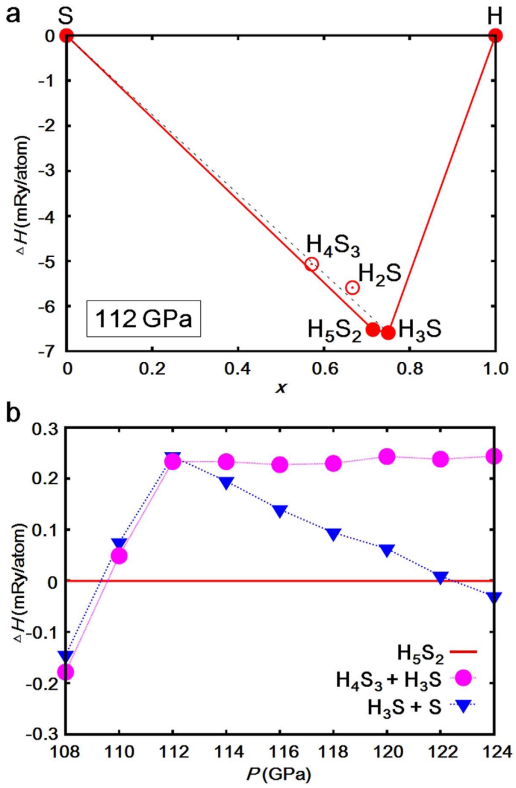

Figure 3. Formation enthalpy per atom as a function of x for H_xS_{1-x} compounds. a, The formation enthalpies of H_4S_3, H_2S, H_5S_2, and H_3S compounds at pressure of 112 GPa. The H_5S_2 and H_3S compounds are on a convex hull shown by solid line, which indicates that the compounds are thermodynamically stable at this pressure. The other compounds are above the convex hull (open circle), which are predicted to be decomposed. b, Pressure dependence of the enthalpies for H_5S_2, $H_4S_3 + H_3S$, and $H_3S + S$. H_5S_2 is composed from H_4S_3 and H_3S at 110 GPa ($H_4S_3 + 7H_3S \rightarrow 5H_5S_2$) and is decomposed into H_3S and S at 123 GPa ($3H_5S_2 \rightarrow 5H_3S + S$).

Discussion

We searched for stable crystal structures of the H_5S_2 stoichiometry, which has hydrogen content between H_2S and H_3S, by the genetic algorithm technique, and found three structures in pressure range from 50 to 250 GPa. H_5S_2 takes the disorderly mixed structure of H_2S and H_2 molecules below 64 GPa, and it transforms into the monoclinic $C2/m$ structure. By further compression, the triclinic $P1$ structure with asymmetric hydrogen bonds formed between H_2S and H_3S emerges above 92 GPa. The convex hull diagram with respect to the H-S compounds shows that $P1$ H_5S_2 is thermodynamically stable in the pressure region from 110–123 GPa. By further compression, $P1$ H_5S_2 is predicted to decompose into $R3m$ H_3S and S: $3\ H_5S_2 \rightarrow 5H_3S + S$.

We calculated the superconducting T_c for $P1$ H_5S_2 and obtained the values of 49.5–71.8 K in pressure region of 100–150 GPa within the harmonic approximation, which shows better superconductivity than P-1 H_2S owing to the large contribution of the H 1s electrons to $N(E_F)$. Errea *et al.* reported the importance of the anharmonicity in sulfur hydrides under high-pressure[9,10]. The anharmonicity hardens H-S stretching modes and softens H-S bending modes, which causes a suppression of λ. As the results, T_c is decreased by approximately 20% (see Table II in ref. 9). In addition, Akashi *et al.* nonempirically determined μ^* as 0.155 for H_2S and 0.168 for H_3S at 130 GPa[11]. Considering these earlier works, we expect that T_c can be corrected to 46.6 K at 112 GPa and 53.2 K at 130 GPa in $P1$ H_5S_2, which are in good agreement with the experimental data for the low-T_c phase (see Table 1). Our predicted $P1$ H_5S_2 is mechanically stable to at least 150 GPa, whereas imaginary phonon frequency appears above the pressure. However, the stable region of the $P1$ H_5S_2 phase is expected to be shifted in higher pressure with the inclusion of the anharmonic effects because the phonon frequency is reported to be pushed up in H_3S owing to the anharmonic effects[9,10]. Therefore, the sharp increase of T_c experimentally observed above 170 GPa in the low-T_c phase[2,3] is probably involved by the structural phase transition from $P1$ or the decomposition of H_5S_2 into H_3S via the intermediate Magnéli phases[19], *i.e.* the transition from the low-T_c phase into the high-T_c phase.

Recently, the x-ray diffraction (XRD) measurements were carried out for H-S system under high-pressure, and $R3m$ H_3S and β-Po S was experimentally confirmed in the high-T_c phase showing $T_c = 203$ K[18]. In the experimental XRD patterns, however, there are some peaks which cannot be identified only by $R3m$ H_3S and β-Po S[18]. We checked whether the unidentified peaks are obtained by our predicted H_5S_2 compound. Figure 7a shows XRD patterns of $R3m$ H_3S, $P1$ H_5S_2, P-1 H_2S, $Pnma$ H_4S_3, and β-Po S at 123 GPa, simulated by RIETAN-2000[22]. The experimental XRD pattern was taken from Fig. 2a of ref. 18, which is obtained by decompression at room temperature after the high-Tc phase is observed at 150 GPa. The wavelength λ of 0.41397 Å was employed for the simulated XRD patterns, which is the same value as the experimental data. The XRD pattern of $P1$ H_5S_2 shows

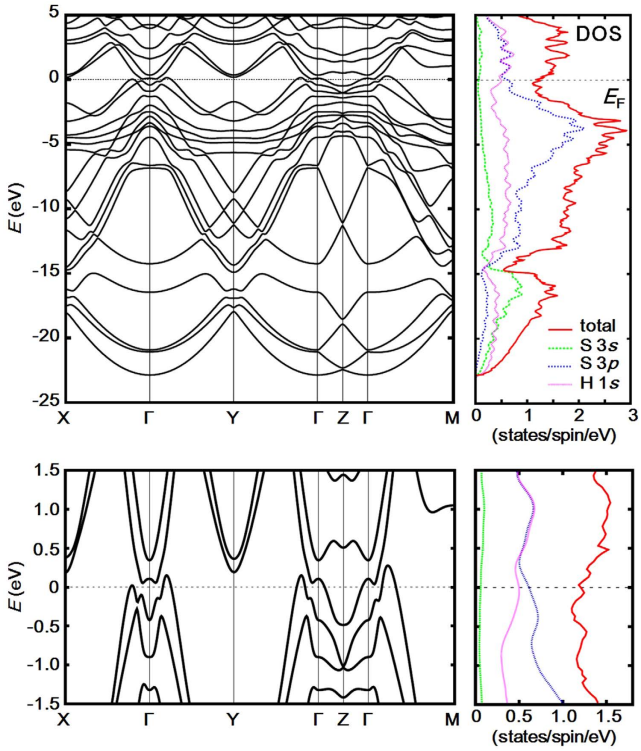

Figure 4. Electronic band structure and density of states (DOS) for *P*1 H_5S_2 at 112 GPa. The lower panel shows a close-up view around the Fermi level (E_F). The calculated band structure forms flat bands near E_F at around the Γ symmetry point and H_5S_2 is a good metal. The partial DOS shows that S 3*p* and H 1*s* are strongly hybridized at E_F.

	P (GPa)	λ	ω_{log} (K)	μ^*	T_c (K)	
H_5S_2	112	1.1856	898	0.13	70.1	
				0.17	58.3	(46.6)
	120	1.2390	907	0.13	75.2	
				0.17	63.2	(50.6)
	130	1.2417	951	0.13	79.1	
				0.17	66.5	(53.2)
H_2S	130	0.77	950	0.13	33	
		0.801	913	0.155	29.4	(23.5)
Exp.	115				30, 50	
	122				40	
	130				55	

Table 1. Superconductivity of *P*1 H_5S_2. Superconducting parameters calculated for *P*1 H_5S_2 within the harmonic approximation: electron-phonon coupling constant λ, logarithmic-averaged phonon frequency ω_{log}, and superconducting critical temperature T_c. Effective screened Coulomb repulsion constant μ^* is assumed to be 0.13 − 0.17. The calculated data for H_2S and experimental data are taken from refs 3, 6 and 11, respectively. The values in parentheses show the T_c values decreased by 20%, which are expected in the calculations with the inclusion of the anharmonic effect.

small diffraction peaks at around $2\theta = 10°$ and at $2\theta = 13°$, which seem to correspond to the unidentified peaks observed in the experimental XRD pattern. However, we cannot clearly conclude that the experimental sample contains *P*1 H_5S_2 owing to the overlapping of many peaks. We also compared the simulated XRD patterns with another experimental data at 121 GPa, taken from Fig. 3(a) of ref. 14 (Fig. 7b). The experimental data is obtained by compression from 10 GPa at room temperature, which is a different experimental protocol from ref. 18. The wavelength λ was set at 0.6199 Å. *P*1 H_5S_2 seems to be included in the experimental XRD data with *Pnma* H_4S_3, while it is hard to explicitly claim the existence of H_5S_2 owing to weak intensity for small peaks in the experimental data. As noted in refs 3 and 14, dissociation products of H_2S depend on pressure-temperature paths. Therefore,

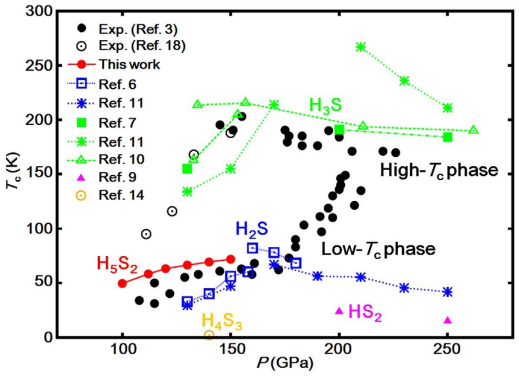

Figure 5. Superconducting critical temperature T_c of the H_5S_2, H_2S, H_3S, H_4S_3, and HS_2 compounds. For H_5S_2, T_c is obtained by the Allen-Dynes formula with the effective screened Coulomb repulsion constant μ^* of 0.17. Calculated T_c data of the other compounds and the experimental data are taken from refs 3, 6, 7, 9, 10, 11, 14 and 18, respectively. The H_5S_2 phase reproduces the experimental data below 170 GPa in the low-T_c phase.

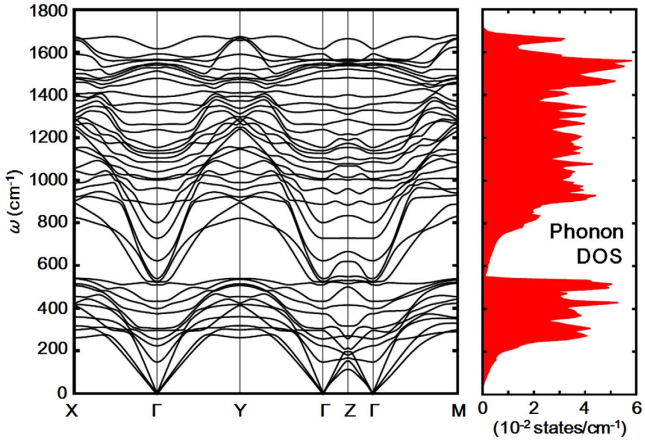

Figure 6. Phonon dispersion curves and density of states for $P1$ H_5S_2 at 150 GPa. $P1$ H_5S_2 is thermodynamically unstable above 122 GPa but is mechanically stable to at least 150 GPa.

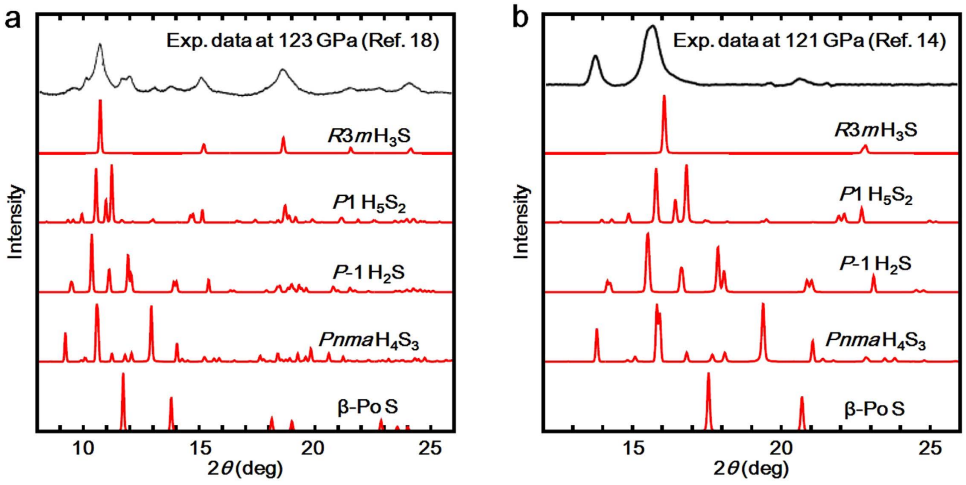

Figure 7. Comparison of x-ray diffraction (XRD) patterns. (**a**) The XRD patterns at 123 GPa are simulated for $R3m$ H_3S, $P1$ H_5S_2, P-1 H_2S, $Pnma$ H_4S_3, and β-Po S with the wavelength λ of 0.41397Å. The experimental data is taken from Fig. 2a of ref. 18, which is obtained by decompression at room temperature after the high-T_c phase is observed at 150 GPa. (**b**) The XRD patterns at 121 GPa are simulated with λ of 0.6199Å. The experimental data is taken from Fig. 3(a) of ref. 14, which is obtained by compression from 10 GPa at room temperature.

the H_5S_2 compound could be observed by further experimental search for optimum pressure-temperature paths to the low-T_c phase.

Methods

We searched for crystal structures by our genetic algorithm (GA) code, which has been developed along the line proposed by Glass *et al.*[23] and been combined with the Quantum ESPRESSO (QE) code[24]. In our GA search, we carried 20 structures in each generation, where 8 structures are created by "crossover", 6 "mutation", and 6 "permutation". We used the simulation cells including 1 to 4 formula units for H_5S_2. Pressures are set at 100, 150, and 200 GPa. The generalized gradient approximation by Perdew, Burke and Ernzerhof[25] was used for the exchange-correlation functional, and the Vanderbilt ultrasoft pseudopotential[26] was employed. The energy cut-off of the plane wave basis was set at 80 Ry. Marzari-Vanderbilt smearing[27] with the width of 0.01 Ry was used for the calculations and the *k*-space integration over the Brillouin zone (BZ) was performed on an $8 \times 8 \times 8$ grid. We increased the number of k-points to a $16 \times 16 \times 16$ grid for the most stable structures obtained through the GA search, which is enough to achieve a convergence within 0.1 mRy/atom in the enthalpy at each pressure.

The superconducting T_c was calculated by the use of the Allen-Dynes formula[28].

$$T_c = \frac{\omega_{\log}}{1.2} \exp\left[-\frac{1.04(1+\lambda)}{\lambda - \mu^*(1+0.62\lambda)}\right].$$

The parameters of electron-phonon coupling constant λ and logarithmic-averaged phonon frequency $\omega_{\log}$ represent a set of characters for the phonon-mediated superconductivity. The softening on the phonon mode is induced by a strong electron-phonon interaction, *i.e.* large λ, resulting in a decrease of $\omega_{\log}$. Therefore, T_c is determined by a balance between λ and $\omega_{\log}$. Using the QE code, we calculated these parameters with a $4 \times 4 \times 4$ *q*-point grid. The *k*-space integration over BZ was performed on a $16 \times 16 \times 8$ grid, and the electron-phonon matrix element at each *q*-point was calculated by a $32 \times 32 \times 16$ grid. The effective screened Coulomb repulsion constant μ^* was assumed to be 0.13–0.17, which is the values nonempirically determined by DFT for superconductors in sulfur-hydrogen system (see Table VI in ref. 11).

References

1. Ashcroft, N. W. Hydrogen Dominant Metallic Alloys: High Temperature Superconductors ? *Phys. Rev. Lett.* **92,** 187002 (2004).
2. Drozdov, A. P., Eremets, M. I. & Troyan, I. A. *Conventional superconductivity at 190 K at high pressures*. Preprint at http://arXiv.org/abs/1412.0460 (2014).
3. Drozdov, A. P., Eremets, M. I., Troyan, I. A., Ksenofontov, V. & Shylin, S. I. Conventional superconductivity at 203 kelvin at high pressures in the sulfur hydride system. *Nature* **525,** 73 (2015).
4. Schilling, A., Cantoni, M., Guo, J. D. & Ott, H. R. Superconductivity above 130 K in the Hg–Ba–Ca–Cu–O system. *Nature* **363,** 56 (1993).
5. Gao, L. *et al.* Superconductivity up to 164 K in $HgBa_2Ca_{m-1}Cu_mO_{2m+2+\delta}$ ($m = 1$, 2, and 3) under quasihydrostatic pressures. *Phys. Rev. B* **50,** 4260(R) (1994).
6. Li, Y., Hao, J., Liu, H., Li, Y. & Ma, Y. The metallization and superconductivity of dense hydrogen sulfide. *J. Chem. Phys.* **140,** 174712 (2014).
7. Duan, D. *et al.* Pressure-induced metallization of dense $(H_2S)_2H_2$ with high-T_c superconductivity. *Sci. Rep.* **4,** 6968 (2014).
8. Duan, D. *et al.* Pressure-induced decomposition of solid hydrogen sulfide. *Phys. Rev. B* **91,** 180502(R) (2015).
9. Errea, I. *et al.* High-Pressure Hydrogen Sulfide from First Principles: A Strongly Anharmonic Phonon-Mediated Superconductor. *Phys. Rev. Lett.* **114,** 157004 (2015).
10. Errea, I. *et al. Quantum Hydrogen-Bond Symmetrization and High-Temperature Superconductivity in Hydrogen Sulfide*. Preprint at http://arXiv.org/abs/1512.02933v1 (2015).
11. Akashi, R., Kawamura, M., Tsuneyuki, S., Nomura, Y. & Arita, R. First-principles study of the pressure and crystal-structure dependences of the superconducting transition temperature in compressed sulfur hydrides. *Phys. Rev. B* **91,** 224513 (2015).
12. Bernstein, N., Hellberg, C. S., Johannes, M. D., Mazin, I. I. & Mehl, M. J. What superconducts in sulfur hydrides under pressure and why. *Phys. Rev. B* **91,** 060511(R) (2015).
13. Heil, C. & Boeri, L. Influence of bonding on superconductivity in high-pressure hydrides. *Phys. Rev. B* **92,** 060508(R) (2015).
14. Li, Y. *et al.* Dissociation products and structures of solid H_2S at strong compression. *Phys. Rev B* **93,** 020103(R) (2016).
15. Bianconi, A. & Jarlborg, T. Lifshitz transitions and zero point lattice fluctuations in sulfur hydride showing near room temperature superconductivity. *Nov. Supercond. Mater.* **1,** 37 (2015).
16. Bianconi, A. & Jarlborg, T. Superconductivity above the lowest Earth temperature in pressurized sulfur hydride. *EPL* **112,** 37001 (2015).
17. Quan, Y. & Pickett, W. E. van Hove singularities and spectral smearing in high temperature superconducting H_3S. Preprint at http://arXiv.org/abs/1508.04491v2 (2015).
18. Einaga, M. *et al. Crystal Structure of 200 K-Superconducting Phase of Sulfur Hydride System*. Preprint at http://arXiv.org/abs/1509.03156v1 (2015).
19. Akashi, R., Sano, W., Arita, R. & Tsuneyuki, S. *Possible "Magnéli" phases and self-alloying in the superconducting sulfur hydride*. Preprint at http://arXiv.org/abs/1512.06680v1 (2015).
20. Luo, H., Greene, R. G. & Ruoff, A. L. β-Po phase of sulfur at 162 GPa: X-ray diffraction study to 212 GPa. *Phys. Rev. Lett.* **71,** 2943 (1993).
21. Pickard C. J. & Needs, R. J. Structure of phase III of solid hydrogen. *Nature Physics* **3,** 473 (2007).
22. Izumi, F. & Ikeda, T. A Rietveld-analysis program RIETAN-98 and its applications to zeolites. *Mater. Sci. Forum* **321-324,** 198 (2000).
23. Glass, C. W., Oganov, A. R. & Hansen, N. USPEX—Evolutionary crystal structure prediction. *Comput. Phys. Comm.* **175,** 713 (2006).
24. Giannozzi, P. *et al.* QUANTUM ESPRESSO: a modular and open-source software project for quantum simulations of materials. *J. Phys.: Condens. Matter* **21,** 395502 (2009).
25. Perdew, J. P., Burke, K. & Ernzefhof, M. Generalized Gradient Approximation Made Simple. *Phys. Rev. Lett.* **77,** 3865 (1996).
26. Vanderbilt, D. Soft self-consistent pseudopotentials in a generalized eigenvalue formalism. *Phys. Rev. B* **41,** 7892 (1990).
27. Marzari, N., Vanderbilt, D., De Vita, A. & Payne, M. C. Thermal Contraction and Disordering of the Al(110) Surface, *Phys. Rev. Lett.* **82,** 3296 (1999).
28. Allen P. B. & Dynes, R. C. Transition temperature of strong-coupled superconductors reanalysed. *Phys. Rev. B* **12,** 905 (1975).

Acknowledgements
This work was supported by JSPS KAKENHI, Grant-in-Aid for Specially Promoted Research (26000006) and Grant-in-Aid for Young Scientists (B) (15K17707).

Author Contributions
T.I., A.N., K.S., H.K.-Y. and N.S. designed the project. T.I. and T.O. developed the genetic algorithm code for crystal structure search, and T.I. performed all the calculations. T.I. wrote the manuscript and all the authors reviewed it.

Additional Information
Competing financial interests: The authors declare no competing financial interests.

How to cite this article: Ishikawa, T. *et al.* Superconducting H_5S_2 phase in sulfur-hydrogen system under high-pressure. *Sci. Rep.* **6**, 23160; doi: 10.1038/srep23160 (2016).